New opportunities in trace elements structural characterization: high-energy X-ray absorption near-edge structure spectroscopy

J. Chaboy,[a]* E. Cotallo,[a] S. Quartieri[b] and F. Boscherini[c]

[a]Instituto de Ciencia de Materiales de Aragón and Departamento de Física de la Materia Condensada, CSIC-Universidad de Zaragoza, 50009 Zaragoza, Spain, [b]Dipartimento di Scienze della Terra, Università degli Studi di Messina, Salita Sperone 31, Contrada Papardo, 98166 Messina-S. Agata, Italy, and [c]Istituto Nazionale per la Fisica della Materia and Dipartimento di Fisica, Università di Bologna, Viale Berti Pichat 6/2, I-40127 Bologna, Italy. E-mail: jchaboy@posta.unizar.es

Garnets in lower crustal mafic and ultramafic rocks usually contain rare-earth elements (REE) in trace concentrations. Direct characterization of REE at trace levels in natural garnets is not available in the literature because of the difficulty of obtaining structural information by means of conventional diffraction methods. Here, the characterization of Nd at trace levels (176–1029 p.p.m.) in a set of natural garnets performed by means of Nd *K*-edge X-ray absorption near-edge structure spectroscopy is presented, showing the capability of high-energy XANES for REE in trace structural determinations.

Keywords: XAS; high energy; trace elements.

1. Introduction

Modern synchrotron radiation facilities provide indispensable tools for research in a large number of different fields of science, such as physics, chemistry and biology, as well as in materials science, geoscience and environmental science. One of the outstanding techniques associated with synchrotron radiation sources is X-ray absorption spectroscopy (XAS). XAS has been demonstrated to be essential to progress in many scientific fields as it provides, by taking advantage of its highly flexible experimental capabilities, knowledge of the local atomic structure of a selected atomic species in the material under study.

Over the last years we have seen the development of the so-called third-generation sources. One of the main challenges within the new facilities connected to XAS is the extension of the available high-energy range. Indeed, the use of XAS as a dedicated tool to determine local structural environments has previously been confined to absorption edges below 30 keV. Recent works have demonstrated that it is possible to measure XAS spectra with sufficiently high signal-to-noise ratios in the energy range 30–90 keV (Braglia *et al.*, 1998; Borowski *et al.*, 1999; Nishihata *et al.*, 1999; Takahashi *et al.*, 1999). The possibility of working at high energy is of significant interest for XAS. For example, in the case of rare-earths most XAS studies are made at the L_3-absorption edge (ranging from 5 to 11 keV), where the presence of the L_2-edge restricts the range of the signal that may be used in an EXAFS analysis to several hundreds of eV. This restriction becomes even higher if some 3*d* transition metal is present in the system under study, as the typical *K*-edge absorption energy for 3*d* metals falls within the same energy interval.

Despite the above advantages there are still only a few works dealing with high-energy XAS and most of them still deal with qualitative and fingerprint analyses. The main reason for this lack of experimental work seems to be linked to the assumption that the finite lifetime of the core-hole smears out dramatically the spectral features so as to avoid structural determination, and that this effect becomes more serious for *K*-absorption edges of heavier elements (Stearns, 1984).

In this work we present the first quantitative analysis made on the X-ray absorption near-edge structure (XANES) region at the Nd *K*-edge in natural minerals containing Nd in trace concentrations. Among the rock-forming minerals, aluminosilicate garnets ($X_3Y_2Si_3O_{12}$, $X = Fe^{2+}$, Mn^{2+}, Mg, Ca) are intensely studied both due to the complexity of their crystal chemistry and to their stability over a wide range of physico-chemical parameters (Merli *et al.*, 1995; Van Westrenen *et al.*, 1999). Garnets in lower crustal mafic and ultramafic rocks usually contain rare-earth elements (REE) in trace concentrations. The diffusion coefficients of REE between garnets and the coexisting phases are used to interpret the crystallization and metamorphic history of crustal rocks. An understanding of REE diffusion in garnets cannot be obtained without a characterization of their structural behaviour. Despite their geochemical importance, a direct crystal chemistry characterization of REE at trace levels in natural garnets is not available in the literature because of the difficulty of obtaining structural information on elements present in such low concentration by means of conventional diffraction methods. The goal of this work is twofold. On the one hand we provide an exact structural determination about the position that Nd enters in the complicated mineral framework. On the other hand we demonstrate the capability of the XANES technique in solving different structural environments, this capability not being affected by the damping and broadening of the signal due to the short lifetime of the excited atomic state.

2. Experimental

We have studied the local environment of Nd at trace levels in a series of natural garnets belonging to the pyrope-grossular solid solution and containing different Nd concentrations (176–1029 p.p.m.). The samples are melanite garnets occurring in carbonatitic rocks: A204 occurs in an alkaline pegmatite from Afrikanda (Kola Karelia), V19 in a jiolite from Vuorijarvi (Kola Karelia) and 89/35 in a jiolite from Potash Sulfur Spring (Arkansas, USA). Samples exhibit different Nd concentration, as determined by ionic microprobe analysis, being 1029, 344 and 176 p.p.m. for A204, V19 and 89/35, respectively. The chemical compositions of the A204, V19 and 89/35 samples are, respectively,

$$X:(Ca_{2.91}Mg_{0.04}Mn_{0.02}Na_{0.03})\ Y:(Mg_{0.10}Ti_{0.89}Zr_{0.04}Al_{0.28}Fe^{3+}_{0.69})\ Z:(Si_{2.34}Fe^{3+}_{0.66})O_{12},$$

$$(Ca_{2.89}Mg_{0.05}Mn_{0.02}Na_{0.04})(Mg_{0.08}Ti_{0.83}Zr_{0.03}Al_{0.20}Fe^{3+}_{0.86})(Si_{2.47}Fe^{3+}_{0.53})O_{12}$$

and

$$(Ca_{2.97}Mn_{0.03}Na_{0.01})(Mg_{0.09}Ti_{0.49}Zr_{0.02}Al_{0.26}Fe^{3+}_{1.14})(Si_{2.66}Fe^{3+}_{0.34})O_{12},$$

with trace concentrations of Ce of 755, 257 and 159 p.p.m., respectively. (The site location of this other REE will be the object of a future study.)

XAS measurements at the commonly used Nd L_3-edge ($\sim$6208 eV) are unattainable in these samples due to the presence of interfering fluorescence lines from the matrix and by the presence of

the Ce L_2-edge (6164 eV) close to the Nd L_3-edge, with a Ce concentration similar to that of Nd. These problems can be overcome by use of the Nd K-edge ($\sim$43570 eV), since at this energy there are no problems of overlapping of absorption edges and fluorescence lines. This energy can be obtained thanks to the high brilliance at high energy of the European Synchrotron Radiation Facility (ESRF) source.

The Nd K-edge spectra were collected at 77 K in transmission mode on the reference compound $Nd(OH)_3$ and in fluorescence mode on powdered samples of the three natural garnets, at the ESRF GILDA BM8 CRG beamline (D'Capito *et al.*, 2002). The Si(511) monochromator was operated in adynamically sagittal-focusing mode (Pascarelli *et al.*, 1996) and harmonic rejection was obtained by detuning the crystals. The energy resolution was about 5.4 eV at 43.5 keV.

A 13-element hyper-pure germanium (HP-Ge) detector was used for the fluorescence measurements; each element is $\sim$10 mm thick, which guarantees that all photons are detected. The signal from each element was processed using a fast digital amplifier and multichannel analyser; a 1 µs peaking time was used and dead-time losses were negligible since the counting rate was of the order of 1000 counts s^{-1} (on each element). In order to filter out the low-energy fluorescence lines originating from the matrix, an Al filter was used (this does not significantly reduce the Nd K_α intensity). At these high energies the main background in the Nd fluorescence comes from rather intense Compton scattering; in fact, the Nd K_α fluorescence accounts only for approximately 1/4 of all the photons reaching the detector.

3. Results and discussion

Fig. 1 reports the raw Nd K-edge XAS spectra for both the reference and the A204 garnet. The XAS oscillations are clearly visible above the edge although, in the case of the garnet, the signal-to-noise ratio beyond $\sim$400 eV above the edge is significantly poorer than in the reference compound (as a consequence of the ultralow Nd concentration in the garnet). However, as shown in Fig. 1, the signal-to-noise ratio for both the $Nd(OH)_3$ and the garnets with Nd content of p.p.m. is comparable at energies close to the absorption edge. Therefore, the Nd K-edge XANES spectra can be used to perform a quantitative determination of the local environment of trace Nd in these garnets. A comparison of the XANES region indicates also that the structural environment of Nd is the same for the three garnets (Fig. 1*b*).

The computation of the XANES spectra was carried out using the multiple-scattering *CONTINUUM* code based on a one-electron full-multiple-scattering theory (Natoli & Benfatto, 1986). The calculation of the Nd K-edge absorption cross sections was performed according to standard FMS methods (Chaboy & Quartieri, 1995). The cluster potential was approximated by a set of spherically averaged muffin-tin (MT) potentials built by following the standard Mattheis' prescription (Mattheis, 1964*a*,*b*). Therefore, the total potential is approximated by a cluster of spherical potentials centred on the atomic sites, and the whole cluster is wrapped by an 'outer sphere'. The radii of the MT potentials centred on the atomic sites were determined following the Norman's criterion and by imposing a 10% overlapping factor (Norman, 1974).

The Coulomb part of each atomic potential was generated using charge densities for neutral atoms obtained from the tabulated atomic wave functions by Clementi & Roetti (1974) and from Herman–Skillman reduced potentials (Herman & Skillman, 1963). The atomic orbitals were chosen to be neutral for the ground-state potential, whereas we follow the $Z + 1$ rule to build the excited-state potential (Lee & Beni, 1977). Finally, an appropriate exchange and correlation (ECP) potential was added to the Coulomb part of the input potential.

Initially we have considered two different possibilities for the position that trace Nd enters in the $X_3Y_2Si_3O_{12}$ garnet structure (Quartieri *et al.*, 1999). Hence, we have built up two class of clusters assuming that Nd enters (i) the dodecahedral X-site and (ii) the octahedral Y-site. In addition, we have always tested the performance of our calculations by using the reference $Nd(OH)_3$.

One of the main steps of the computation is to determine the minimum size of the cluster needed to reproduce all the structures present in the experimental XANES spectra. To this end we performed different calculations increasing progressively the number of atoms in the built-up cluster. In the case of the reference $Nd(OH)_3$, new absorption features are found by increasing the coordination shells around the photoabsorbing Nd atom up to $\sim$5 Å. No differ-

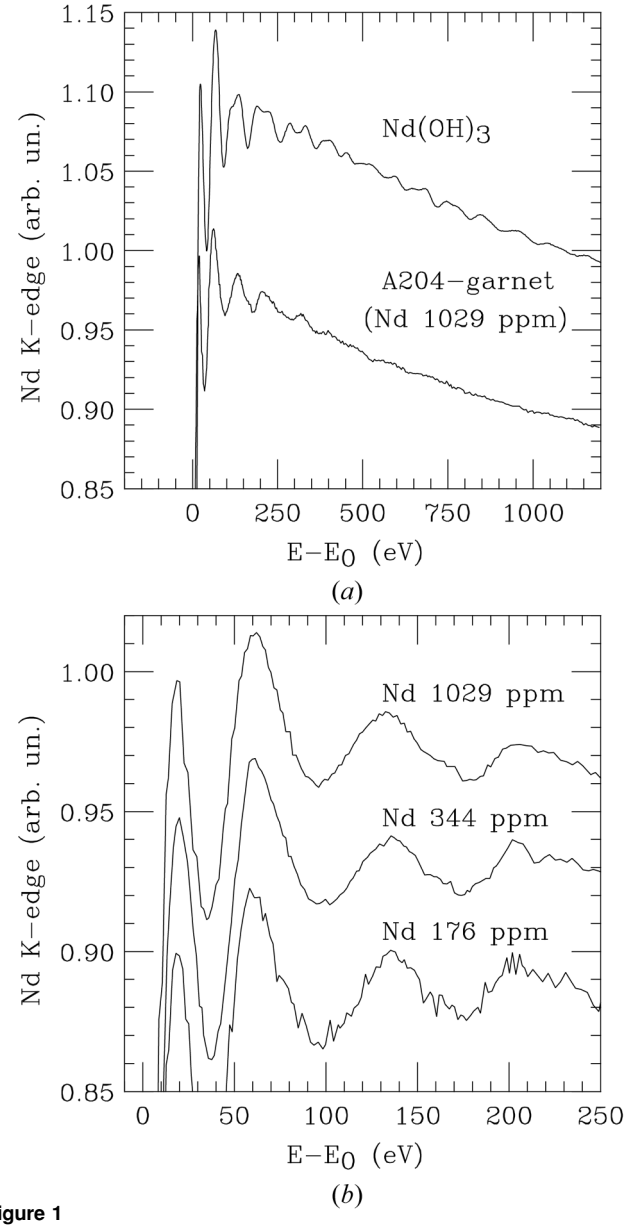

Figure 1
(*a*) Raw Nd K-edge absorption spectra of $Nd(OH)_3$ and melanite garnet with an Nd content of 1029 p.p.m. (A204). (*b*) Detailed comparison of the XANES region for the three garnets under study.

ences are found between the 5.4 Å and 6.7 Å clusters, indicating that further coordination shells do not contribute significantly to the XANES. Similar results are found for the case of the Nd *K*-edge in garnets, both at the *X*-site and the *Y*-site. This means that the spectral features shown in Fig. 1 are due to multiple-scattering processes of the photoelectron and neighbouring atoms located within a sphere of ~5 Å radius around the central Nd.

Once the cluster size has been fixed for both the reference and trace Nd systems, we have computed the Nd *K*-edge XANES spectra by using different ECP potentials (Chaboy & Quartieri, 1995; Quartieri *et al.*, 1999). In the case of the reference compound, results of the computation are rather satisfactory for real Hedin–Lundqvist potentials. Theoretical spectra reproduce all the features present in the experimental spectra, the relative intensity of the different absorption features as well as their relative energy separation. The use of this ECP potential leads to the best reproduction of the relative intensity of the absorption features. It should be noted that, when using the X_α or the Dirac–Hara potentials, the energy separation between the various spectral features is not completely satisfactory. Indeed, the energy scale of the theoretical X_α (Dirac–Hara) spectrum is contracted (expanded) with respect to that of the experimental spectra. In addition, the use of the complex Hedin–Lundqvist potential induces an excessive damping of the multiple-scattering contribution to the spectra. After taking into account the effect of the core-hole lifetime (17.3 eV; Krause & Oliver, 1979) and the experimental resolution, the agreement between the computation and the experimental XANES is remarkable, as shown in Fig. 2.

The same procedure has been applied to the natural garnets. Fig. 3 shows a comparison between the Nd *K*-edge XANES spectrum of the garnet with an Nd content of 1029 p.p.m. (A204) and the theoretical computations performed by assuming that Nd enters the octahedral and dodecahedral sites. It should be noted that the energy scale of each computation is referred to its own muffin-tin potential so that calculation provides a unique energy scale to align both *X*- and *Y*-site theoretical spectra. The results of the computation strongly suggest that trace Nd enters the dodecahedral *X*-site. The same comparison made after convolution of the theoretical spectra with the full core-hole width not only validates this result but also shows convincingly that the structural determination is not affected by the damping and broadening of the signal due to the short lifetime of the excited atomic state.

Summarizing, the study of the high-energy *K*-edge X-ray absorption of Nd occurring in trace concentrations in natural garnets demonstrates that Nd enters a structural garnet site and does not occupy matrix defects. Indeed, Nd enters the dodecahedral X-site of the $X_3Y_2Si_3O_{12}$ garnet structure and does not substitute Al at the octahedral *Y*-site. Therefore, we provide a direct crystal chemistry characterization of rare-earth elements at trace levels in natural

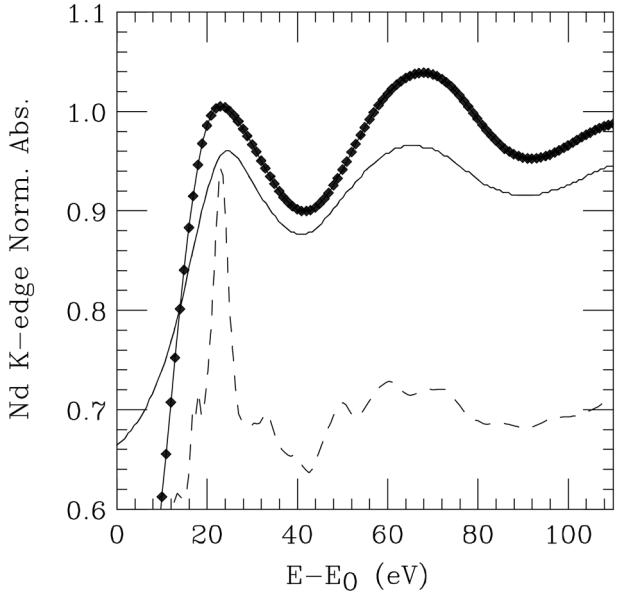

Figure 2
Comparison between the experimental Nd *K*-edge XANES signal of $Nd(OH)_3$ and the computation prior to (dashed) and after (solid line) the convolution taking into account the full Nd *K*-edge core-hole width.

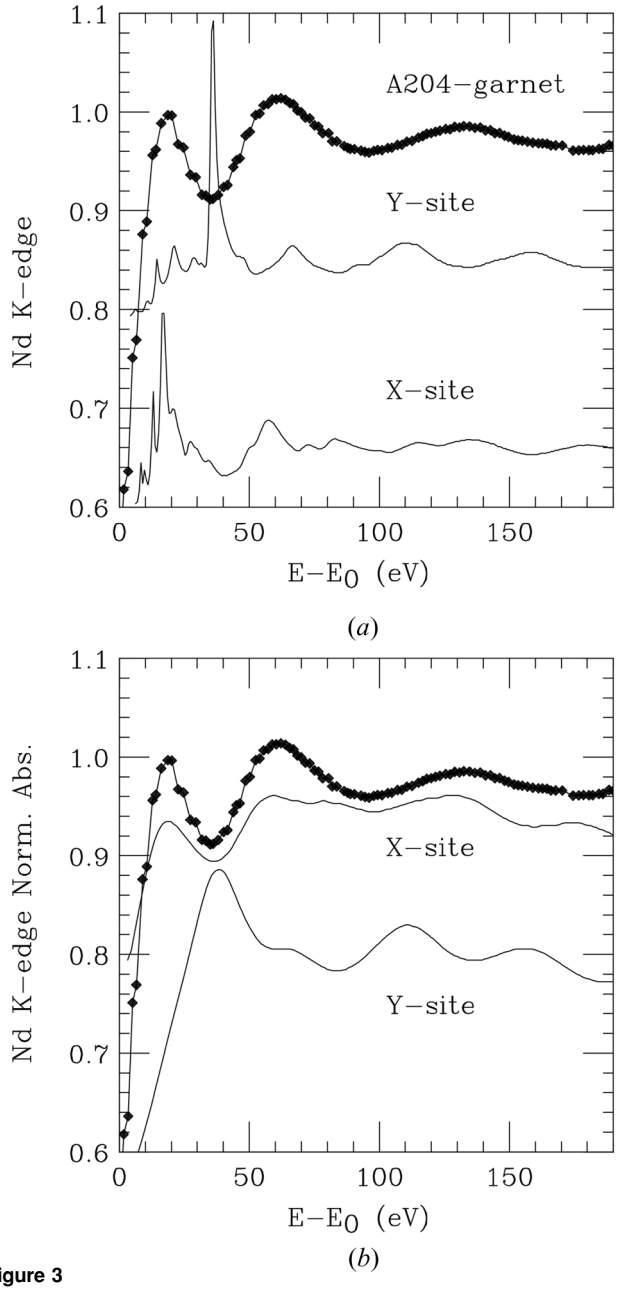

Figure 3
(*a*) Comparison between the experimental Nd *K*-edge XANES signal of A204 and those calculated on the basis of the FMS theory assuming Nd in the dodecahedral (*X*-site) or in the octahedral (*Y*-site) sites. (*b*) The same comparison as (*a*) after the convolution of the computation by taking into account the full Nd *K*-edge core-hole width.

garnets, not available in literature. Moreover, the capability of high-energy XANES as a powerful structural tool providing structural details unattainable by using standard methods has been demonstrated.

This work was partially supported by the Aragón DGA P0004/2001, Spanish DGICYT MAT99-0667-C04-04 and Italian MURST (COFIN99 transformations, reactions, ordering in minerals) grants. Financial support for the experimental work at the ESRF was provided by the ESRF 'Public User Program'.

References

Borowski, M., Bowron, D. T. & De Panfilis, S. J. (1999). *J. Synchrotron Rad.* **6**, 179–181.
Braglia, M., Dai, G., Mosso, S., Pascarelli, S., Boscherini, F. & Lamberti, C. (1998). *J. Appl. Phys.* **83**, 5065–5068.
Chaboy, J. & Quartieri, S. (1995). *Phys. Rev. B*, **52**, 6349–6357.
Clementi, E. & Roetti, C. (1974). *Atom. Data Nucl. Data Tables*, **14**, 177–478.
D'Acapito, F., Colonna, S., Maurizio, C. & Mobilio, S. (2002). *J. Synchrotron Rad.* **9**, 24–27.
Herman, F. & Skillman, S. (1963). *Atomic Structure Calculation.* Englewood Cliffs, NJ: Prentice-Hall.
Krause, M. O. & Oliver, J. H. (1979). *J. Phys. Chem. Ref. Data*, **8**, 329–338.
Lee, P. A. & Beni, G. (1977). *Phys. Rev. B*, **15**, 2862–2883.
Mattheis, L. F. (1964*a*). *Phys. Rev. A*, **133**, 1399–1403.
Mattheis, L. F. (1964*b*). *Phys. Rev. A*, **134**, 970–973.
Merli, M., Callegari, A., Cannillo, E., Caucia, F., Leona, M., Oberti, R. & Ungaretti, L. (1995). *Eur. J. Miner.* **7**, 1239–1249.
Natoli, C. R. & Benfatto, M. (1986). *J. Phys. (Paris) Colloq.* **47**(C8), 11–23.
Nishihata, Y., Emura, S., Maeda, H., Kubozono, Y., Harada, M., Uruga, T., Tanida, H., Yoneda, Y., Mizuki, J. & Emoto, T. (1999). *J. Synchrotron Rad.* **6**, 149–151.
Norman, J. G. (1974). *Mol. Phys.* **81**, 1191–1198.
Pascarelli, S., Boscherini, F., D'Acapito, F., Hrdy, J., Meneghini, C. & Mobilio, S. (1996). *J. Synchrotron Rad.* **3**, 147–155.
Quartieri, S., Chaboy, J., Antonioli, G. & Geiger, C. A. (1999). *Phys. Chem. Miner.* **27**, 88–94.
Stearns, D. G. (1984). *Philos. Mag. B*, **49**, 541–558.
Takahashi, M., Harada, M., Watanabe, I., Uruga, T., Tanida, H., Yoneda, I., Emura, S., Tanaka, T., Kimura, H., Kubozono, Y. & Kikkawa, S. (1999). *J. Synchrotron Rad.* **6**, 222–224.
Van Westrenen, W., Blundy, J. & Wood, B. (1999). *Am. Mineral.* **84**, 838–847.

 Received 14 November 2001 • Accepted 4 February 2002